IL NUOVO CIMENTO **45 C** (2022) 77
DOI 10.1393/ncc/i2022-22077-8

COMMUNICATIONS: SIF Congress 2021

ReD dual-phase, liquid argon time projection chamber

G. MATTEUCCI

Dipartimento di Fisica "Ettore Pancini", Università degli Studi di Napoli Federico II Naples, Italy

received 31 January 2022

Summary. — Within the DarkSide project, the ReD (Recoil Directionality) experiment was set up to study and characterize the performance of a double-phase argon Time Projection Chamber (TPC), testing for directional sensitivity and response to very low energy nuclear recoils. The TPC of ReD was characterized at INFN Napoli with γ and neutron sources, to evaluate its performances in various conditions. This article presents the main results obtained during the characterisation campaign.

1. – Introduction

The dark matter puzzle and DarkSide. – In the last century, a great number of astronomical observations have led to the hypothesis of dark matter: a form of non-baryonic matter which interacts with ordinary particles (primarily) via gravitational force. It is estimated, in particular by the analysis of the Cosmic Microwave Background (CMB), that dark matter is the most abundant form of matter in the Universe [1]. However, the true nature of dark matter is still unresolved, despite the huge efforts made by physicists. One of the most accredited hypotheses for the nature of dark matter is that it is composed of a yet undiscovered Weakly Interacting Massive Particle (WIMP), not part of the Standard Model of particle physics, which would constitute a cold dark matter candidate. WIMPs could be detected in an experiment through collisions with ordinary matter. Even though mass and cross section are left as free parameters of the theory, the parameter region not constrained by astronomical and cosmological observations allows only for an extremely small collision rate, in the form of nuclear recoils with low recoiling energies (1–100 keV, assuming a WIMP mass of 10–1000 GeV/c^2 [2]). This prediction sets the requirements for high exposure ultra-low background detectors for direct search experiments.

The DarkSide project was created to test the WIMP hypothesis with dual-phase argon time projection chambers (LAr TPCs) as physics detectors. The first of the DarkSide series of experiments is DarkSide-50, with an active volume of about 50 kg of liquid argon. It was run at Laboratori Nazionali del Gran Sasso (LNGS) from 2013 to 2020, limiting the allowed region in the cross section and mass parameter space for a WIMP candidate [3, 4]. It will be succeeded by DarkSide-20k (DS-20k), which is being designed and will be assembled in the following years. DS-20k will have an active mass of about 50

tons of liquid argon, resulting in a 1000-fold increased exposure compared to DarkSide-50. The construction of a detector of such sensitivity to probe lower cross section values requires lower background levels. For this reason, radiopure Silicon Photomultipliers (SiPMs) will be used as photosensors and underground argon (UAr) will be used as the active medium of the TPC. UAr has a naturally occurring low abundance of the radioactive isotope ^{39}Ar [5], which is a dangerous source of background.

The neutrino floor and directional discrimination. – Nevertheless, DarkSide-20k and similar detectors in the next decade will suffer from an unprecedented type of background as the exposure of those experiments is increased. At cross sections of the order of $10^{-49}\,\mathrm{cm}^2$ (for a WIMP with mass $m = 10$–$100\,\mathrm{GeV}/c^2$) coherent elastic neutrino-nucleus scattering is predicted to become a sizable source of background. Such interactions produce mostly recoils with energies much lower than the one expected from a WIMP-induced recoil, but the fraction of events with higher energy becomes significant as experiments probe rarer events. This kind of interaction is virtually indistinguishable from a WIMP-nucleus interaction, posing a limit to the search for dark matter. This background is usually referred to as *neutrino floor.*

New methods for particle discrimination are needed to search for dark matter below the neutrino floor. One promising technique involves the measurement of the incident particle (neutrino or WIMP) direction. For both dark matter and neutrino events, a privileged incident direction is expected. For neutrinos, this direction is known to be the one joining laboratory with their sources: two fluxes of neutrinos are expected to come from the Sun (produced in nucleosynthesis processes) and from the atmosphere (produced by interactions with cosmic rays). For WIMPs, the standard halo model predicts an isotropic distribution of velocities, decoupled from the galactic rotational motion. This implies a *wind effect*, with a greater flux of WIMPs from the direction towards which the Solar System is pointing with its revolution motion around the galactic centre.

If one were able to measure the direction of the incoming particle in a direct search experiment, this information could be used to discriminate statistically between a WIMP or a neutrino event.

ReD: Recoil Directionality. – The Recoil Directionality (ReD) experiment is born within the DarkSide Collaboration with this experimental aim: the testing of a measurable directional effect in LAr TPCs detectors and, eventually, the characterisation of such directional response. A theoretical basis is found in the columnar recombination model [6]. LAr TPCs extract information on the recoil by measuring both the scintillation and ionisation produced by an event in the active medium. These develop two signals, usually referred to as S1 and S2, respectively. S1 and S2 both depend on the recombination rate of electron-ion pairs produced by an event; a higher recombination rate results in more scintillation and less ionisation (as fewer charge carriers are left to produce a ionisation signal). Electrons need to be drifted towards an amplification region via an electric field (drift field) to extract the S2 signal. The columnar recombination model predicts a dependence for the S2/S1 ratio on the angle of the recoil with respect to the electric field permeating the medium. As the angle varies, so does the fraction of electron-ion pairs which recombine, resulting in anti-correlation between the intensity of the signals S1 and S2 for a fixed energy.

It has been shown in [7] that for a recoiling argon nucleus, the expected WIMP interaction would preserve the directional information, while a hint for a directional effect is found in [8] by the SCENE Collaboration. In their study, nuclear recoils in a LAr TPC

were tagged by parallel or orthogonal direction with respect to the electric drift field. The S1 signal exhibited an orientation difference, but with marginal statistical significance. The authors concluded that a higher sensitivity experiment was needed to clarify the situation. The directional anti-correlation between the ionisation and scintillation signals could be measured by any dual-phase LAr TPC detector with enough resolving power (including DS-20k TPC) with no prior modification to the system, due to such an effect being dependent only on the active medium, the electric field, and the kind and energy of the interaction.

The verification of a measurable directional response for LAr TPCs in the energy interval of interest is the main focus of ReD. The experiment was set up with two additional goals in mind: the testing of SiPMs performance and stability in a cryogenic environment and the characterisation of LAr TPCs response to very low energy nuclear recoils ($\lesssim$1 keV). This last point will not be discussed in the present work.

ReD setup and first results. – The experimental setup for ReD is designed to detect neutron recoils in a LAr TPC tagged at different angles with respect to the electric field, but with the same scattering angle, in a closed kinematic system. Nuclear recoils of known energy and direction are produced by irradiating the TPC with a neutron beam. A monoenergetic lithium beam produced by the Tandem accelerator at Laboratori Nazionali del Sud (Catania) is directed towards a CH_2 target in a vacuum scattering chamber to produce neutrons via the nuclear reaction p(^{7}Li,^{7}Be)n. A fraction of the emitted neutrons travels towards the TPC, where neutrons interact with the active medium and scatter. Those exiting the TPC with an angle of 36.8° with respect to the beam direction are tagged by a neutron spectrometer made by an array of liquid scintillator detectors (LSci). Each LSci tags a neutron-induced nuclear recoil with a different angle to the electric field, so that a directional dependence of the signal can be directly observed. Different recoil energies are obtained by varying the lithium beam energy.

At present, the ReD experiment has already taken the first batch of measurements, and the obtained data is being analyzed. In this article, the most relevant results from the TPC calibration campaign, carried out at INFN Naples, are presented. The collaboration has recently published all the information relevant to the characterisation of the TPC in a paper [9]; figures and results are reported in this article with the kind permission of The European Physical Journal (EPJ).

2. – ReD TPC

Description and mode of operation. – The core detector of the ReD experiment is a dual-phase liquid argon TPC, which implements some of the features planned for the DS-20k TPC, on a smaller scale. The active region is a cuboid with dimensions 5 cm × 5 cm × 6 cm ($l \times w \times h$). A hexagonal stainless steel mesh placed at 5 cm from the bottom separates the drift region (a 125 cm^3 cube) from the upper charge amplification region. The walls of the active volume contain a sheet of Enhanced Specular Reflector (ESR), sandwiched between two layers of acrylic plastic for structural support. The bottom and ceiling of the cuboid are enclosed by two acrylic windows deposited with a conductive layer of indium tin oxide (ITO) on both sides. All the internal surfaces are also deposited with a wavelength shifter material, tetraphenyl butadiene (TPB), to accommodate for the response curve of the photosensors used (SiPMs). Two tiles of twenty-four SiPMs each are placed adjacent to the windows. Each tile is directly connected to a custom made front end board. In single-phase mode, the whole volume

of the active chamber is filled with liquid argon. Only the scintillation signal produced by excitation and recombination of ionized argon nuclei are observed in an event. In dual-phase mode, a voltage difference is applied to an external resistor (boiler) to boil some of the argon. Gaseous argon flows to the upper region of the inner cuboid (called the diving bell), while escape holes on the walls of the detector keep the liquid-gas interface at a 3 mm level above the mesh. To produce an electric field, a voltage difference is applied on both the ITO internal layers on the acrylic windows and on the mesh, while the external ITO layers are grounded for insulation. An array of copper rings placed around the detector and supplied by a voltage divider is used to improve the homogeneity of the drift field within the active volume. This configuration allows for the decoupling of the electric field in the liquid region and diving bell. In a dual-phase event scenario, the S1 signal is produced in the same matter as single-phase mode, although a quenching effect is induced by the electric field reducing the recombination ratio. A fraction of the electrons produced by ionisation is drifted across the mesh. A stronger field in the proximity of the grid allows extracting electrons from the liquid to the gas phase. In gaseous argon, the intense electric field causes the electrons to produce secondary photons by electroluminescence. The electroluminescence photons are detected by the SiPMs and their number is proportional to the number of electrons extracted from the liquid. The signal produced this way is referred to as S2. Due to the proximity of the electroluminescence effect to the top SiPM tile, the S2 signal is used to obtain information on the horizontal position of the event. The time interval between S1 and S2 signals (defined as drift time) is used to measure the vertical position of the event, as the drifting electrons produced further from the grid take longer to reach it. A render of the TPC is presented in fig. 1, while a labelled photograph of it is shown in fig. 2. A typical waveform illustrating the scintillation and ionisation signals is shown in fig. 3.

Silicon photomultipliers, readout system. – The SiPMs used by ReD are customized for the DarkSide project and developed by Fondazione Bruno Kessler (FBK). The photon detection efficiency is maximum for wavelength of $\sim$420 nm ($>$50% at room temperature). They are characterized by a triple doping concentration, 25-μm cell pitch and 10 MΩ quenching resistance (at cryogenic temperature). Each tile contains 24 SiPMs; on the bottom tile, they are summed in groups of six, while on the top board each SiPM is read out individually to improve horizontal spatial resolution. This choice is justified by the electroluminescence production happening very close to the top window. Two custom

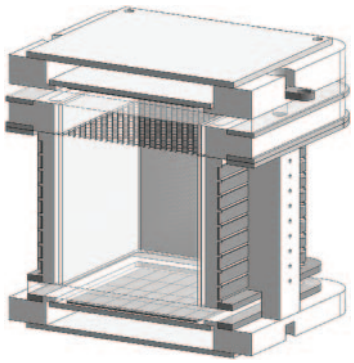

Fig. 1. – Digital rendering of ReD TPC cut open, revealing the active volume. Taken from [9].

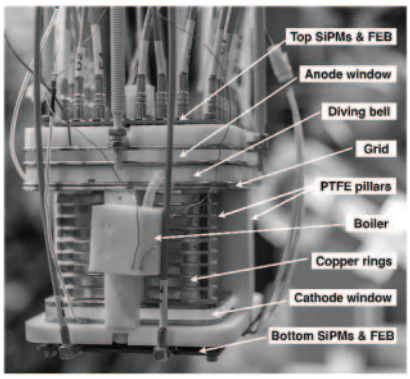

Fig. 2. – Picture of the TPC with labeling to highlight the distinct elements. Taken from [9].

made Front-End Boards (FEBs) are used to supply power to the photosensors, to amplify the output signals with a low-noise amplifier, and to sum over 6 SiPMs channels (bottom FEB only). Each SiPM is operated at a fixed bias voltage of 34 V, corresponding to 7 V of overvoltage with respect to the breakdown voltage.

Cryogenic system. – The cryogenic system containing the TPC is responsible for the condensation (filling mode) and maintenance (recirculation mode) of the liquid argon. The argon is supplied to the system from a research-grade gaseous argon (N6.0) bottle, but in recirculation mode the argon gas source is excluded and any evaporated argon is purified by a SAES hot getter before being recondensed. As a consequence, argon purity is constantly increasing as the system runs in a closed loop. A LabView-written, slow control software is used to operate the system remotely and to acquire data from the sensors involved to be stored in a database.

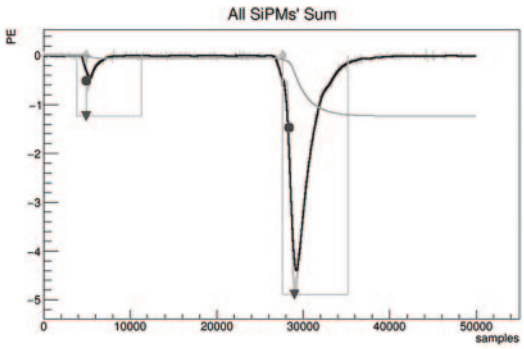

Fig. 3. – Typical waveform of an event seen by the ReD TPC. The two signals S1 and S2 are both respectively visible as the first pulse and second pulse (dark solid line, which is a running average of the raw signal visible as the lighter underlying trace). The boxes around the two signals highlight the work of the peak finding algorithm, while the smoother solid line is the integrated signal.

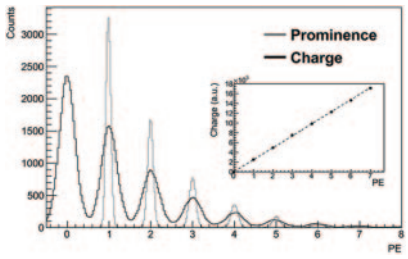

Fig. 4. – Distribution of events per charge measured for a top tile in a laser calibration run, scaled to number of photoelectrons corresponding to each peak, for both charge integration and prominence methods. Inset: charge *vs.* photoelectron number, fitted with a linear function to retrieve the SER value. Taken from [9].

3. – Results of the characterisation campaign

The characterisation campaign for the TPC was taken at the INFN "CryoLab" laboratory at the University of Naples Federico II. The system has operated continuously between 7 June 2019 and 18 November 2019, for 165 days. In this article, only the most relevant results are presented. Detailed information about the analysis and performed measurements, along with specific characteristics for each component of the system, are available in [9]. In this section, the main results will be presented for the following tests: SiPM response to single photon, energy calibration, scintillation (and ionisation) response for nuclear and electronic recoils, purity measurement. All the plots presented in this section are sourced from [9] as well.

SiPM response to single photoelectron. – To evaluate SiPM Response to Single photoElectron (SER) an external 50 ps pulsed, 403 nm laser is let shine into the cryostat via a feedthrough. A bunch of dispersed optical fibres inside the cryostat scatter the light to expose each SiPM to a qualitatively uniform fraction of photons. Calibration runs of this kind were performed regularly to evaluate SiPMs stability in the cryogenic environment and to update corrections for relative variations of the response between different SiPMs. The charge is measured offline for each readout channel by integrating the digitized waveform; a second analysis is carried out on the same data by applying a digital filter to the waveform. By deconvoluting the SiPM response function and then measuring the height of the filtered peak (and summing heights for multiple peaks), produced charge information can be extracted with greater resolution, but the filtering process is much more CPU intensive. The sum of peak heights is defined as prominence.

The distribution of hits per value of integrated charge and prominence is presented for a top SiPM in fig. 4. The corresponding charge values are shifted so that the first peak (pedestal peak) in the integrated charge distribution is located at $N_{PE} = 0$ hits. The prominence distribution instead does not show a pedestal peak, since prominence can only be measured from events with at least one pulse. Each peak corresponds to a different number of photoelectrons detected by the SiPM. In the insert, the mean value for each peak is plotted *vs.* the corresponding number of photoelectrons: SER is obtained as the slope of a linear fit for these variables, as the mean charge produced per photoelectron. The standard deviation σ_1 of the peak corresponding to one photoelectron is 0.16 (0.20) PE for the charge distribution of bottom (top) channels. As stated before, prominence can significantly improve resolution at the cost of greater computational effort. Using the prominence method $\sigma_1 = 0.076$ (0.057) PE for the bottom (top) tile.

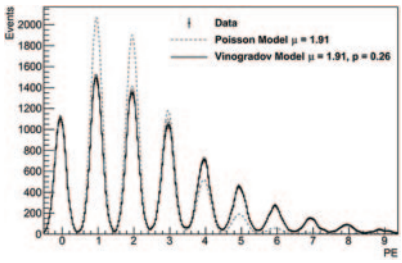

Fig. 5. – Distribution of events per charge measured for a top tile in a laser calibration run. The data is fitted with the Vinogradov model and superimposed with a Poissonian distribution graphed with the same mean value for primary photoelectron emission as the one obtained from the Vinogradov fit. Taken from [9].

Crosstalk and afterpulse effects. – SiPMs suffer from crosstalking (CT) and afterpulsing (AP). In a crosstalk event, a hit provoked by a photon on the SiPM induces adjacent cells to discharge too, resulting in a higher number of photoelectrons measured for a single initial photon. In an afterpulse event, a single cell produces more than one discharge per primary photon due to electrons being trapped by impurities or lattice defects, and producing a new avalanche after being released. These phenomena are accounted for with statistical analysis. For an ideal SiPMs tile that is not affected by CT/AP, the probability of measuring N photoelectrons should be distributed in a Poissonian fashion. In the case of CT/AP, such probability does not follow a Poissonian distribution and it is shifted toward higher values. A better-suited model is the Vinogradov model [10], which uses a compound Poissonian distribution. By running a maximum likelihood fit on the amplitude distribution, values are obtained for the mean number of primary photoelectrons (μ) and probability for a primary photoelectron to produce a secondary emission (p). A coefficient of duplication is defined as $K_{dup} = p/(1-p)$, so that the value $(1 + K_{dup})$ represents the total number of photoelectrons detected for each primary photoelectron. A typical fit is shown in fig. 5, corresponding to the solid line. The dotted line corresponds to a Poissonian distribution with the same mean value as the μ parameter obtained with the corresponding compound Poissonian distribution. Typical values for K_{dup} range between 0.31 and 0.37 between different channels, with statistical uncertainties from the fit of approximately 3% for each channel.

SER and K_{dup} fluctuations. – The relative fluctuations of the SER values, calculated through the 165-day long campaign, is 0.7% (1.0%) rms for bottom (top) channels. This effect is compatible with the fluctuations in the output voltage of the power supply feeding the SiPMs. The relative fluctuations of the K_{dup} parameter for each channel are 3.0% (3.6%) rms for bottom (top) channels, within the uncertainties of the individual fits.

Energy calibration. – Response of the TPC both in single-phase mode and double-phase mode were studied using an external ^{241}Am source, emitting γ-rays at $E_\gamma = 59.54\,\text{keV}$, producing electron recoils. In single-phase mode, as mentioned in the previous section, the fields are turned off and the chamber is full of liquid argon. Only the S1 signal is produced. In double phase mode, the detector is fully functional and two signals are produced. The light yield (LY) is defined as the number of photoelectrons produced per unit of energy. Registered events are corrected for a geometrical asymmetry dependent on the event z position, called Top Bottom Asymmetry (TBA), before

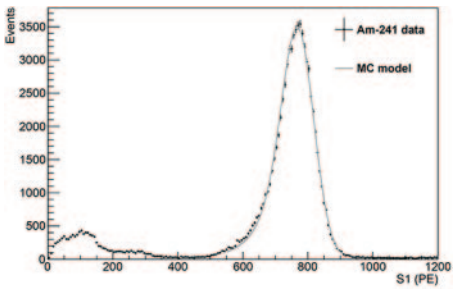

Fig. 6. – The S1 spectrum for a ^{241}Am calibration run, fitted with a Monte Carlo model. The peak corresponds to the γ emission at 59.54 keV. Light yield is obtained from the fit results. Taken from [9].

measuring the LY. The value for LY already corrected for TBA is referred to as Y_{raw}. Another correction is necessary to account for the effect of CT/AP. The corrected light yield is obtained by $Y_{corr} = Y_{raw}/(1 + \langle K_{dup} \rangle)$. The value for Y_{raw} is obtained by fitting the distribution of events produced by the ^{241}Am source with a Monte Carlo model. For null field configuration (single-phase mode), the measured spectrum is shown in fig. 6, from which a value of $Y_{1,corr} = (9.80 \pm 0.13)$ PE/keV is obtained (the $_1$ subscript refers to the scintillation signal S1). The resolution for the ^{241}Am spectrum is measured to be $\sigma/\mu = 6.4\%$ (6.6% without TBA correction). Four runs of this kind were taken in equivalent conditions throughout the operational period to evaluate time stability; the position of the ^{241}Am peak is reproducible to within 2% among those runs. Other sources with emissions that produce electron recoils with different energies were used to test the linearity of the response. The measurements for light yield are all compatible within uncertainties. Light yield at null field was also measured with the gas pocket turned on, producing a negligible variation.

S1 and S2 anti-correlation. – The experimental gains for S1 and S2, g_1 and g_2 respectively, can be measured from the correlation between S1 and S2. Following the procedure found in [8], light yield for S1 and S2 can be expressed by $Y_1 = b - a \cdot Y_2$, where a and b are constants from which the gains g_1 and g_2 can be derived. Y_1 and Y_2 can be varied by changing the drift field in the active region, as the fraction of recombining electron-ion pairs depends on the intensity of the charge-drifting field, which in turn influences the respective yields $Y_{1,2}$. The data obtained by following such procedure is reported in fig. 7, and the following values are measured for the gains: $g_1 = (0.195 \pm 0.018)$ PE/photon and

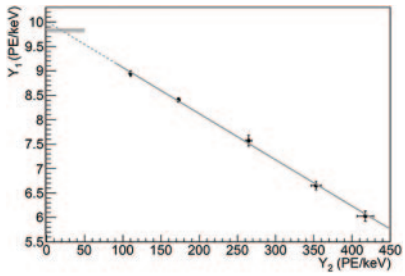

Fig. 7. – Anti-correlation between S1 and S2 signals (their respective light yields are plotted). The horizontal bar corresponds to the null field configuration data point, as S2 is not measurable. Taken from [9].

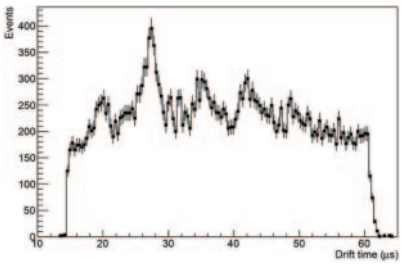

Fig. 8. – Drift time distribution for a ^{241}Am run. The peaks and valleys trend is caused by the copper ring structure partially shielding the source-emitted radiation. Taken from [9].

$g_2 = (20.7 \pm 1.6)$ PE/e$^-$. The results obtained are comparable with those from DarkSide-50 ($g_1^{DS50} = (0.157 \pm 0.001)$ PE/photon and $g_2^{DS50} = (23 \pm 1)$ PE/e$^-$, from [4,11]), proving that ReD satisfies the requirements needed to achieve its scientific goals.

Drift time, drift velocity and electron lifetime. – Drift time is defined as the temporal difference between S1 and S2 and contains information about the z coordinate of the event. In fig. 8 the distribution in drift time is shown for events produced by a ^{241}Am source with an electric drift field of $E_d = 183\,\mathrm{V/cm}$. The distribution cuts off at $\sim 62\,\mu$s, which corresponds to the time needed for an electron produced on the bottom of the active chamber to reach the amplification region. No event is present for drift time smaller than $\sim 12\,\mu$s as S1 and S2 signals overlap and the reconstruction algorithm fails to process the event. Electron drift velocity can be measured from the maximum value of the drift time and dimensions of the chamber, then compared to literature to test for electric field uniformity. In the full paper [9], two different parameterisations are fitted to drift velocities obtained in ReD for different values of the electric field, leaving the argon temperature as a free parameter; the fit shows good agreement with data and the obtained temperature is compatible with the actual temperature measured by sensors placed inside the cryostat.

Electrons drifting towards the amplification region, after being produced in an event, can be captured by electronegative contaminants dispersed in the argon, such as oxygen and nitrogen. The number of electrons decreases exponentially with a time constant τ defined in this scenario as electron lifetime. Ideally, electron lifetime should be much greater than maximum drift time for a particular field configuration, so that only a small variation is produced on the S2 signal due to electron capture. Electron lifetime is evaluated by an exponential fit of the mean value for S2 (normalized to S1) *vs.* the drift time. This is presented in fig. 9, for a ^{241}Am calibration run with an electric drift field

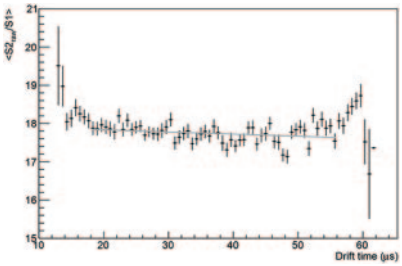

Fig. 9. – S2/S1 plotted against drift time for a ^{241}Am run. A slowly decreasing dependence is observed, due to electron capture, from which electron lifetime is estimated. Taken from [9].

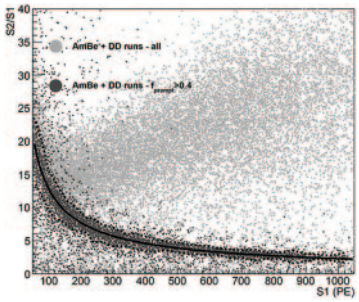

Fig. 10. – Distribution of nuclear recoils (darker data points) compared to all events (lighter data points) in the S2/S1 *vs.* S1 for the AmBe and deuterium-deuterium sources combined dataset. Mean value of S2/S1 for nuclear recoils is plotted as the solid line, with the black dashed curves representing the 90% C.L. Taken from [9].

value of 183 V/cm. This run was taken after 37 days of continuous argon recirculation, and a value of $\tau = (1.8 \pm 0.6)$ ms is measured. It has been observed that after a week of recirculation, electron lifetime is greater than 1 ms; in this scenario, the correction applied to S2 is at the level of a few per cent.

Particle discrimination and response to nuclear recoils. – The ReD TPC was exposed to two neutron sources during the characterisation campaign: an AmBe source and a commercial deuterium-deuterium neutron generator. LAr TPCs can discriminate between nuclear recoils (produced neutrons and expected from a WIMP interaction) and electronic recoils (mainly produced by charged particles) by two means: pulse shape discrimination and S2/S1 ratio. Pulse shape discrimination is carried out by evaluating the f_{prompt} parameter for each event, defined as the fraction of an S1 signal produced in a defined time interval at the start of the event. The scintillation processes of argon show a measurable difference for electronic or nuclear recoils, modifying the shape of the signal. The time interval is chosen to maximise discrimination power and was set to be 700 ns in ReD. The difference in S2/S1 is instead mainly attributed to recoiling nuclei producing a denser ionisation cloud compared to recoiling electrons, resulting in more recombination, and so a smaller S2/S1 ratio.

Since ReD aims to characterize a directional effect that produces a variation in the S2/S1 ratio, S2/S1 resolution is a key parameter for the success of the experiment. In fig. 10, a scatter plot for S2/S1 *vs.* S1 is drawn for combined events from all neutron sources, with two samples differentiated by a cut in f_{prompt}. The darker data points correspond to nuclear recoil events and are located at smaller S2/S1 values. The mean value and width of S2/S1 are calculated in intervals of S1 with a varying width between 20 and 40 PE, as shown in fig. 11. The measured dispersion is measured to be 12% in the energy range 150-200 PE, showing good uniformity across the considered energy intervals. This resolution is sufficiently high to ensure that a potential directional effect with a magnitude equal to that suggested by the results from SCENE would not be hidden by instrumental resolution. In this regard, the performance of the TPC reported here meets the requirements needed to accomplish the main goals of the ReD experiment.

4. – Conclusions

The ReD TPC has been thoroughly characterized in Naples, calibrating the key parameters of the system to maximise the resolution for nuclear recoils (NRs). The ex-

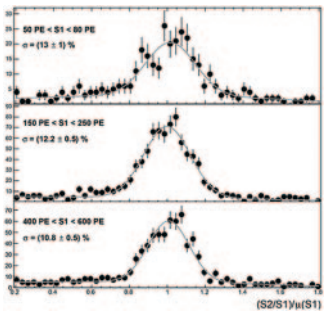

Fig. 11. – Distribution of $(S2/S1)/\langle(S2/S1)\rangle$ in three energy ranges: 50–80 PE (top panel), 150–250 PE (middle panel), and 400–600 PE (bottom panel). The measured widths are reported for each panel, obtained by fitting a model consisting of a Gaussian distribution summed with a linear function. Taken from [9].

perimental requirements to observe a directional effect have been accomplished and the system was shipped to INFN LNS (Laboratori Nazionali del Sud), where it has already undergone the first campaign of data taking, currently under analysis by the ReD team. The observed good stability of SiPMs response for a long period (six months) of continuous operation in a cryogenic environment is a promising result towards the transition to radiopure silicon photosensor technology for future high-exposure high-sensitivity dark matter direct search experiments.

* * *

I would like to thank my supervisor Prof. Giuliana Fiorillo for the support and the valuable guidance she provided me since I joined the "CryoLab" Laboratory in Naples, as well as Dr. Luciano Pandola, Dr. Yury Suvorov, Dr. Simone Sanfilippo for the help and patience shown during the last few years. My sincere appreciation goes to the ReD research group and to everyone at "CryoLab" Laboratory for allowing me to partake in the lab activities.

REFERENCES

[1] Aghanim N. *et al.*, *Astron. Astrophys.*, **641** (2020) A6.
[2] Lewin J. and Smith P., *Astropart. Phys.*, **6** (1996) 87.
[3] DarkSide Collaboration (Agnes P. *et al.*), *Phys. Rev. D*, **98** (2018) 102006.
[4] DarkSide Collaboration (Agnes P. *et al.*), *Phys. Rev. Lett.*, **121** (2018) 081307.
[5] Xu J. *et al.*, *Astropart. Phys.*, **66** (2015) 53.
[6] Jaffé G., *Ann. Phys.*, **374** (1913) 303.
[7] Cadeddu M. *et al.*, *JCAP*, **01** (2019) 014.
[8] SCENE Collaboration (Cao H. *et al.*), *Phys. Rev. D*, **91** (2015) 092007.
[9] Agnes P. *et al.*, *Eur. Phys. J. C*, **81** (2021) 1014.
[10] Vinogradov S. *et al.*, *IEEE Nucl. Sci. Symp. Conf. Rec.*, **25** (2009) 1496.
[11] Agnes P. *et al.*, *JINST*, **12** (2017) P10015.